Stress distribution near the diffusion bonding interface of Fe$_3$Al and Cr18-Ni8 stainless steel

Y. Li*, C. Xia, J. Wang

Key Laboratory for Liquid-Solid Structural Evolution and Processing of Materials (Ministry of Education),
School of Materials Science and Engineering, Shandong University,
Jinan 250061, P. R. China

Abstract

The stress distribution of Fe$_3$Al/Cr18-Ni8 stainless steel diffusion bonding joint was calculated, the method of numerical simulation and thermo-elastic-plastic finite element method (FEM) were adopted. The results indicated that the stress peak value appeared near the interface of Cr18-Ni8 steel side. This is the key factor inducing crack. With increasing of the heating temperature and time, the stress of Fe$_3$Al/Cr18-Ni8 diffusion bonding joint increased. The largest stress value with a heating temperature of 1100 °C is about 65.9 MPa, which is higher than the stress peak value at 1000 °C by 9.4 %. For a certain arrangement of thickness, the stress is becoming larger with the increasing of the thickness of test plate. When the thickness is beyond a certain critical value (about 8 mm), the stress varies slightly with the thickness.

K e y   w o r d s: Fe$_3$Al intermetallic, dissimilar materials, diffusion bonding, stress finite element method (FEM)

1. Introduction

Fe$_3$Al intermetallic has many merits, such as excellent wear, oxidation and corrosion resistance and low cost, and receives considerable concerns from researchers [1–5]. Consequently, solving the welding problem of Fe$_3$Al intermetallic and Cr18-Ni8 stainless steel can get their respective advantages in terms of performance and economy. This is a critical technique for the application of Fe$_3$Al intermetallic as a high temperature structural material in the fields of petrochemical and electric power industries. Thus, the hydrogen brittleness [6] and thermal stress at the joint generated during welding Fe$_3$Al intermetallic cause the appearance of welding crack and poor weldability, which seriously limits the application of Fe$_3$Al as structural material. At present, critical progress has been acquired in the research of the welding Fe$_3$Al and stainless steel [7], however, the research of stress distribution of the Fe$_3$Al/Cr18-Ni8 diffusion bonding joint has been rarely reported until now.

Because of the differences of heat expansion coefficient and microstructure of Fe$_3$Al intermetallic and Cr18-Ni8 stainless steel, there is complex stress appearance near the weld joint, which is the important factor leading to the welding crack. However, it is almost impossible to measure the stress distribution of the diffusion bonding joint exactly. In this paper, the stress distribution near the interface of Fe$_3$Al/Cr18-Ni8 diffusion bonding joint is calculated and the effect of heating temperature and thickness of matrix to the stress of Fe$_3$Al/Cr18-Ni8 steel diffusion bonding joint is researched, with the method of numerical simulation and thermo-elastic-plastic finite element method (FEM) adopted. The variety of major thermal-physical properties of materials with technology parameter is considered. This research will provide theoretical and experimental bases for the application of Fe$_3$Al/Cr18-Ni8 dissimilar materials.

2. Experimental

Experimental materials were Fe$_3$Al intermetallic

---

*Corresponding author: tel./fax: +86-531-88393538; e-mail address: yj23699@163.com

T a b l e 1. Thermal-physical properties of Fe₃Al and Cr18-Ni8 steel used in the calculation

Materials	Temperature T (°C)	Coefficient of heat expansion α (10^{-6} K^{-1})	Young's modulus E (GPa)	Thermal conductivity λ (W m^{-1} °C^{-1})	Volume specific heat C (J kg^{-1} °C^{-1})
	100	15	140	12.5	599
	200	17	–	13.3	610
	300	18	–	14.2	680
Fe₃Al	400	23	–	15.15	750
	500	26	–	16	850
	600	25.5	–	17.15	800
	700	27	–	18	800
	20	–	184	16.3	502
	100	16.6	–	–	–
	200	17.0	–	17.6	–
	300	17.2	–	18.8	–
18-8	400	17.5	159	20.5	–
Stainless steel	500	17.9	–	21.8	–
	600	18.2	137	23.5	–
	700	18.6	120	24.7	–
	800	–	88	26.4	–
	900	–	–	28.5	–

Note: Density of Fe₃Al, $\rho = 6.72$ g cm^{-3}, tensile strength $\sigma_b = 455$ MPa, Poisson's ratio $\mu = 0.3$;
density of 18-8 stainless steel, $\rho = 7.9$ g cm^{-3}, tensile strength $\sigma_b = 520$ MPa, Poisson's ratio $\mu = 0.3$.
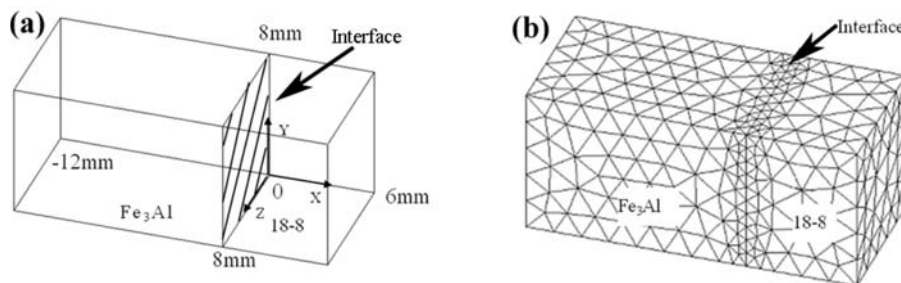

Fig. 1. Schematic diagram of the diffusion bonding joint and mesh division of finite element method (FEM): (a) the schematic diagram of diffusion bonding joint, (b) mesh division of FEM.

and Cr18-Ni8 austenitic stainless steel (1Cr18Ni9Ti). The Fe₃Al intermetallic was melted in a vacuum induction furnace and then fabricated into plate, and treated under uniform annealing at 1000 °C. Fe₃Al and Cr18-Ni8 steel were welded together by advanced vacuum diffusion bonding. The sizes of samples were: Fe₃Al intermetallic 12 mm × 8 mm × 8 mm; Cr18-Ni8 stainless steel 8 mm × 8 mm × 6 mm. The process parameters of the diffusion bonding were: the heating temperature 1000–1100 °C, the holding time 15–60 min, the pressure 10–20 MPa, the vacuum degree 1.33×10^{-4} Pa. The schematic diagram of the diffusion bonding joint and coordinates is shown in Fig. 1a.

The analysis of stress for the Fe₃Al/Cr18-Ni8 diffusion bonding joint belongs to the high-temperature thermo-elastic-plastic problem. Thermal physical properties of Fe₃Al and Cr18-Ni8 steel used in the calculation are shown in Table 1. The difference of heating expansion and cooling shrinkage near the interface of Fe₃Al/Cr18-Ni8 diffusion bonding joint causes change

of the thermal stress. In this paper, the stress distribution near the interface of the diffusion bonding is analysed, using the method coupling thermal and structure properties. The finite element model is built up according to the size of test plate. In order to get accurate calculation results, the model is refined near the interface of the diffusion bonding where the stress is larger. The division of the finite element mesh in the FEM calculation is shown in Fig. 1b.

The course of finite element analysis for the stress distribution of Fe₃Al/Cr18-Ni8 diffusion bonding joint is shown in Fig. 2. The initial temperature of model is set to the heating temperature of vacuum diffusion bonding, and the ending temperature is set to the room temperature after cooling, then the stress distribution from the heating temperature to the room temperature is calculated. Setting different initial temperature according to different heating temperature, the stress distribution under different heating temperature separately is calculated. Flow of finite element
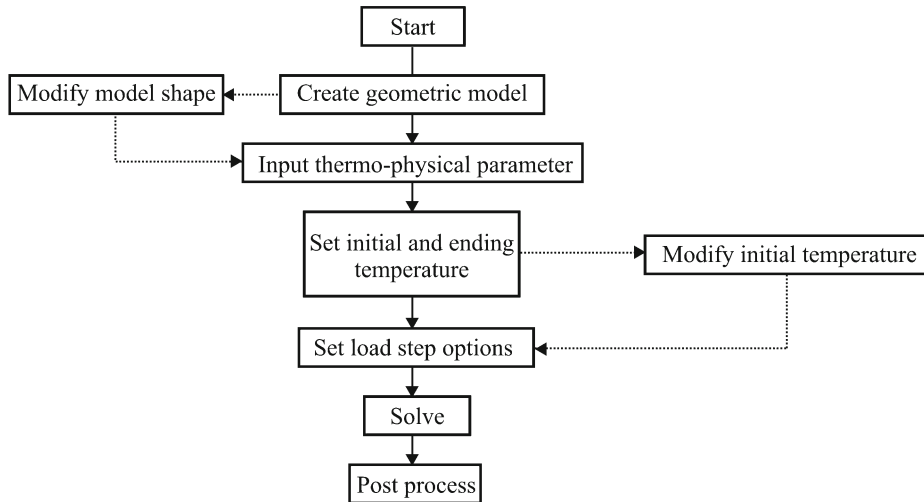
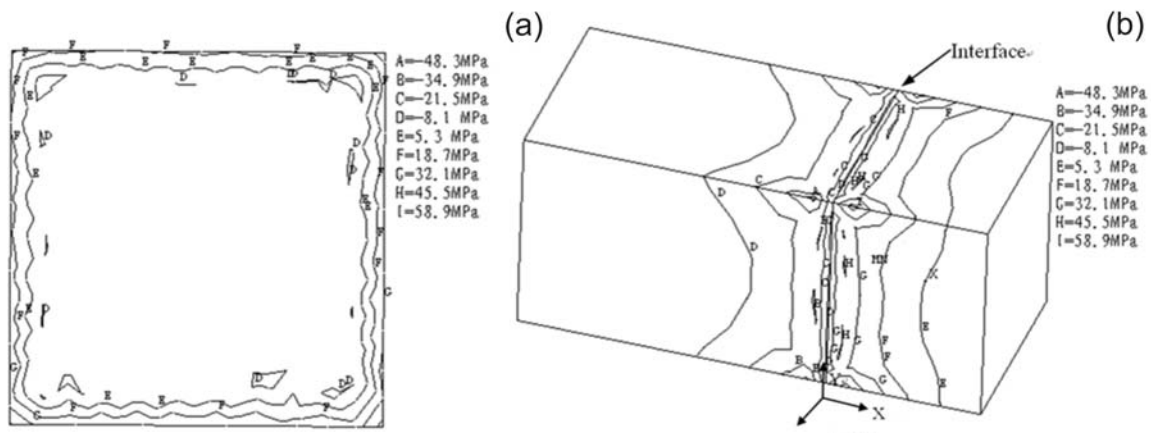Fig. 2. Flow of finite element analysis of the stress distribution.

Fig. 3. X-axis stress distribution at the bonding interface: (a) cross-section, (b) surface.

calculation of the stress distribution is shown with dotted line in Fig. 2.

3. Results and analysis

3.1. Stress distribution of Fe₃Al/Cr18-Ni8 diffusion bonding joint

The axial (X direction) stress distribution near the interface is shown in Fig. 3a,b, and all the curves in the figures are stress constant value lines, and the words on the lines stand for the stress values. From Fig. 3a, it can be seen that the further the distance from central axis of the sample interface is, the larger the stress is, and the largest stress appears on the sample surface.

The axial (X direction) stress distribution of the sample surface is shown in Fig. 3b. From Fig. 3b it can be seen that the peak value of stress appears in a narrow zone of both sides of the interface (near 0.8 mm for both sides from the interface). This result is corresponding to the broken position of actual diffusion bonding joint, which mostly appears in the zone on both sides of the interface [8]. The largest stress is on the edges of both sides of the interface. On the Fe₃Al side, the stress performs as compressive stress, and the largest stress value is about 48.3 MPa, which is about 10.6 % of Fe₃Al tensile strength (455 MPa). On the Cr18-Ni8 steel side, the stress performs as tensile stress, and the largest stress value is about 58.9 MPa, which is about 11.3 % of the tensile strength of Cr18--Ni8 steel (520 MPa). The joint easily tends to appear crack and then break at this position under a tensile stress.

From Fig. 3a, it also can be seen that the variety of stress near the diffusion interface is larger, the change of stress on different position near the interface is apparent, the stress constant value line fluctuation is larger comparatively, and the stress concentration is obviously on the edge of sample. From Fig. 3b, it can be seen that the stress constant value lines are distributed densely near the interface, which indicates
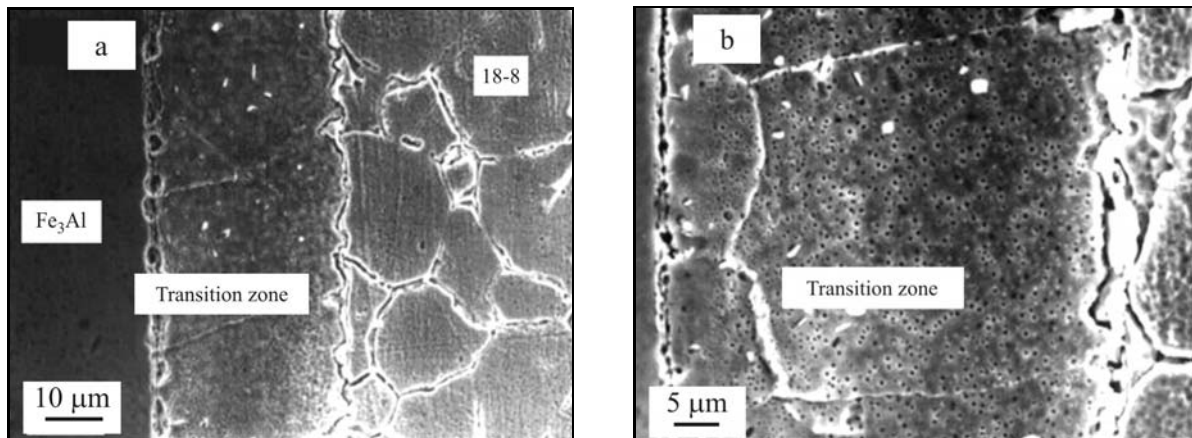
Fig. 4. Microstructure near the interface of Fe$_3$Al/18-8 diffusion bonding: (a) 1000×, (b) 2000×.
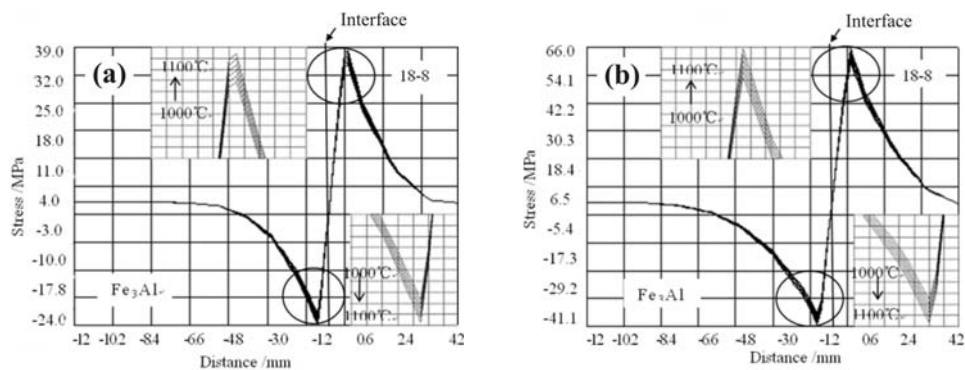

Fig. 5. Stress distribution near the Fe$_3$Al/Cr18-Ni8 diffusion bonding interface: (a) bonding surface perpendicular to interface, (b) edge perpendicular to interface.

that the gradient of stress distribution near the interface is larger, and the variety of stress is apparent. Microstructure near the Fe$_3$Al/Cr18-Ni8 diffusion interface is shown in Fig. 4. It is seen from Fig. 4 that in the interface transition zone of the Fe$_3$Al side the density changes comparatively, while in the interface transition zone of the Cr18-Ni8 steel side micro-cracks appear. It is because the coefficients of heat expansion of Fe$_3$Al and Cr18-Ni8 steel are different, and that larger stress appears on the Cr18-Ni8 steel side near the diffusion bonding interface after the sample cooling. This is corresponding to the calculated results of stress distribution near the interface.

3.2. Effect of heating temperature and thickness of the sample on stress distribution

The heating temperature and time should be strictly controlled when Fe$_3$Al and Cr18-Ni8 steel dissimilar materials are welded by the vacuum diffusion bonding. The heating temperature has great influence on the stress near the diffusion interface. The property of the diffusion bonding joint varies greatly under different heating temperature. The stress distribution

near the interface under different heating temperatures ranging from 1000 ℃ to 1100 ℃ is shown in Fig. 5. The stress distribution at the bonding surface perpendicular to the interface is shown in Fig. 5a, and stress distribution at the edge perpendicular to the interface is shown in Fig. 5b.

When the heating temperature changes from 1000 ℃ to 1100 ℃, the stress at the same position near the interface gets larger (Fig. 5). The higher the heat temperature, the larger the stress near the interface is. The largest stress appears with a heating temperature at 1100 ℃. The amplitude of the compressive stress at bonding surface perpendicular to the interface is about 2.8 MPa (Fig. 5a), which is about 9 % of the largest compressive stress (31.0 MPa). The amplitude of the tensile stress at bonding surface perpendicular to the interface is about 3.5 MPa, which is about 9 % of the largest tensile stress (38.9 MPa). From Fig. 5b, it can be seen that the amplitude of the compressive stress at the sample edge perpendicular to the interface is about 4.7 MPa, which is about 9 % of the largest compressive stress (52.9 MPa). The amplitude of the tensile stress at the sample edge perpendicular to the interface is about 6.2 MPa, which is about 9.4 % of the
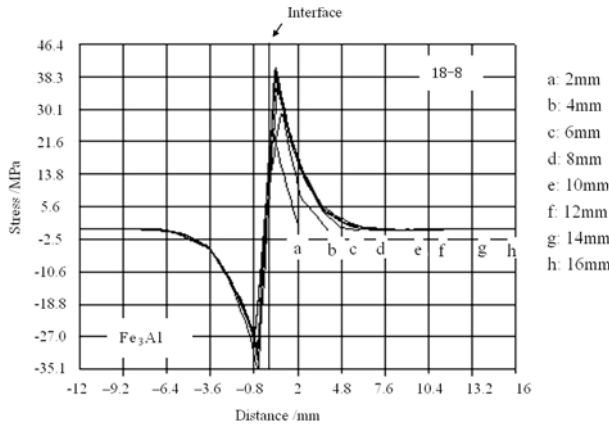
Fig. 6. Effect of thickness of Cr18-Ni8 steel on stress distribution at bonding surface perpendicular to interface.

largest tensile stress (65.9 MPa). Therefore, the stress of the diffusion bonding joint varies greatly with the changing of the heating temperature.

The shape of sample affects the stress distribution greatly comparatively, too. In order to analyse the effect of thickness of a sample on the stress distribution of diffusion bonding joint, the stress distribution near the interface was calculated in this paper separately when the thickness of Cr18-Ni8 steel increased from 2 mm to 16 mm. With a constant 12 mm thickness of Fe_3Al and different thickness of Cr18-Ni8 steel, the effect of thickness of Cr18-Ni8 steel on the stress distribution at the diffusion bonding surface perpendicular to the interface is shown in Fig. 6.

In Fig. 6 (a–h), these curves are separately stress distribution lines at diffusion bonding surface perpendicular to the interface when the thickness of Cr18-Ni8 steel increases from 2 mm to 16 mm. From Fig. 6, it can be seen that with the increase of the thickness of Cr18-Ni8 steel, the stress increases on the Fe_3Al side, but the amplitude is still small. When the thickness changes from 2 mm to 8 mm, the stress on the Cr18-Ni8 steel side increases obviously (from 25.2 MPa to 39.1 MPa); when the thickness changes from 8 mm to 16 mm, the stress changes slightly (from 39.1 MPa to 40.1 MPa). According to the above analysis, with the increase of thickness of sample, the stress near the interface of the Cr18-Ni8 steel side increases, but when the thickness changes to a critical value (8 mm), the stress increases slightly, and when the thickness increases continually (more than 8 mm), the stress near the interface of the side of Cr18-Ni8 steel tends to a constant value, which will not change any more.

4. Conclusions

1. The stress distribution near the diffusion bonding interface of Fe_3Al/Cr18-Ni8 steel dissimilar materials indicates, that the further the distance from the central axis of the interface is, the larger the stress is, and the largest stress appears on the surface of the joint sample. The gradient of the stress distribution near the interface is larger.

2. The zone of apparent stress variety is in the zone of 5 mm from both sides of the interface, and the stress reaches the peak value at the 8 mm from both sides of the interface. Furthermore, the largest stress value is on the Cr18-Ni8 steel side.

3. With the increasing of heating temperature and time, the stress increases gradually. When the heating temperature changes from 1000 °C to 1100 °C, the largest stress value is about 65.9 MPa, which is larger than the stress peak value at 1000 °C by about 9.4 %. In a certain arrangement of thickness, the stress is becoming larger with the increasing of the sample thickness. When the thickness is beyond a certain critical value (about 8 mm), the stress varies slightly with thickness.

References

[1] Hotař, A., Kratochvíl, P., Hotař, V.: Kovove Mater., *47*, 2009, p. 247.
[2] Li, J. N., Chen, C. Z., Lin, Z. Q., Squartini, T.: J. Alloy Compd., *509*, 2011, p. 4882. doi:10.1016/j.jallcom.2011.01.199
[3] Karlík, M., Kubošová, A., Haušild, P., Prahl, J.: Kovove Mater., *46*, 2008, p. 77.
[4] Pešička, J., Karlík, M.: Kovove Mater., *42*, 2004, p. 275.
[5] Li, J. N., Chen, C. Z., Zong, L.: Inter. J. Refract. Met. Hard Mater., *29*, 2011, p. 49.
[6] Castagna, A., Stoloff, N. S.: Mater. Sci. Eng., *192/193A*, 1995, p. 399. doi:10.1016/0921-5093(94)03240-8
[7] Wang, J., Li, Y. J., Yin, Y. S.: Materials Science Research India, *1*, 2003, p. 1.
[8] Li, Y. J., Wang, J.: Mater. Sci. Technol., *12*, 2004, p. 45.